

## Spaceborne measurements of atmospheric CO<sub>2</sub> by high-resolution NIR spectrometry of reflected sunlight: An introductory study

Zhiming Kuang,<sup>1</sup> Jack Margolis,<sup>2</sup> Geoffrey Toon,<sup>2</sup> David Crisp,<sup>2</sup> and Yuk Yung<sup>1</sup>

Received 30 October 2001; revised 12 February 2002; accepted 12 February 2002; published 2 August 2002.

[1] We introduce a strategy for measuring the column-averaged CO<sub>2</sub> dry air volume mixing ratio  $X_{\text{CO}_2}$  from space. It employs high resolution spectra of reflected sunlight taken simultaneously in near-infrared (NIR) CO<sub>2</sub> (1.58- $\mu\text{m}$  and 2.06- $\mu\text{m}$ ) and O<sub>2</sub> (0.76- $\mu\text{m}$ ) bands. Simulation experiments, show that precisions of  $\sim 0.3$ –2.5 ppmv for  $X_{\text{CO}_2}$  can be achieved from individual clear sky soundings for a range of atmospheric/surface conditions when the scattering optical depth  $\tau_s$  is less than  $\sim 0.3$ . When averaged over many clear sky soundings, random errors become negligible. This high precision facilitates the identification and correction of systematic errors, which are recognized as the most serious impediment for the satellite  $X_{\text{CO}_2}$  measurements. We briefly discuss potential sources of systematic errors, and show that some of them may result in geographically varying biases in the measured  $X_{\text{CO}_2}$ . This highlights the importance of careful calibration and validation measurements, designed to identify and eliminate sources of these biases. We conclude that the 3-band, spectrometric approach using NIR reflected sunlight has the potential for highly accurate  $X_{\text{CO}_2}$  measurements. **INDEX TERMS:** 0322 Atmospheric Composition and Structure: Constituent sources and sinks; 0394 Atmospheric Composition and Structure: Instruments and techniques; 1640 Global Change: Remote sensing

### 1. Introduction

[2] Reliable predictions of future levels of atmospheric CO<sub>2</sub> require a quantitative understanding of both CO<sub>2</sub> emissions and the specific processes and reservoirs responsible for sequestering CO<sub>2</sub> [IPCC, 1996]. Measurements from a surface network are currently used to monitor atmospheric CO<sub>2</sub>. While these measurements are highly accurate, the network is too sparse to adequately characterize the geographic distribution of the CO<sub>2</sub> sinks and the processes controlling their variability [Sarmiento and Wofsy, 1999]. As a result, spaceborne techniques are being sought to measure the column averaged CO<sub>2</sub> with more complete global coverage.

[3] To surpass the performance of the existing surface network for inferring sources and sinks of atmospheric CO<sub>2</sub>, inversion studies suggest that a precision of better than 2.5 ppmv is needed for global measurements of monthly mean column-averaged CO<sub>2</sub> dry air volume mixing ratio or vmr ( $X_{\text{CO}_2}$ )<sup>1</sup> on a  $8^\circ \times 10^\circ$  grid [Rayner and O'Brien, 2001]. In addition, because sources and sinks are inferred from spatial and temporal gradients in  $X_{\text{CO}_2}$ , these measurements must have no significant geographically varying biases. Here, we introduce a method to measure  $X_{\text{CO}_2}$  from space, and use simulated spectra to demonstrate that high precisions can be achieved. We briefly review the effects of systematic errors and biases, but defer a more comprehensive investigation to later publications.

<sup>1</sup>Division of Geological and Planetary Sciences, California Institute of Technology, Pasadena, CA, USA.

<sup>2</sup>Jet Propulsion Laboratory, California Institute of Technology, Pasadena, CA, USA.

### 2. Measurement Strategy

[4] To produce self-consistent estimates of retrieval precision, all results presented here are based on simulations of a practical satellite instrument design, which employs three spectrometers that simultaneously take high resolution spectra of reflected sunlight in near-infrared (NIR) CO<sub>2</sub> and O<sub>2</sub> bands (Figure 1).

[5] The 1.58- $\mu\text{m}$  CO<sub>2</sub> band is well suited for retrieving column CO<sub>2</sub> because it is virtually free of interfering atmospheric absorptions, and is also sufficiently weak that the continuum level can be ascertained between the CO<sub>2</sub> lines even at high solar zenith angles (SZAs), with a power ( $R = \lambda/\Delta\lambda$ ) of about 21,000 (i.e., the spectral resolution is about 0.075 nm). This facilitates the detection of wavelength-dependent variations of the surface albedo or airborne cloud and aerosol particles.

[6] Spectra of the 1.58- $\mu\text{m}$  CO<sub>2</sub> band alone, however, cannot yield  $X_{\text{CO}_2}$  with sufficient precision, because space-based measurements of the absorption in this band are influenced by a number of factors besides the CO<sub>2</sub> vmr. Uncertainties in the surface pressure and the atmospheric path traversed by the reflected radiation can contribute errors in  $X_{\text{CO}_2}$ . Both topographic variations over land and local weather contribute uncertainties in surface pressure and total atmospheric mass in a CO<sub>2</sub> sounding. Scattering by clouds/aerosols further contribute to uncertainties in the atmospheric pathlength. Undetected water vapor variations introduce uncertainties in  $X_{\text{CO}_2}$ , both by altering the dry-air fraction of the total atmospheric pressure, and by broadening the CO<sub>2</sub> lines more efficiently than O<sub>2</sub> and N<sub>2</sub>. All these factors must be explicitly constrained to retrieve  $X_{\text{CO}_2}$  to the required high precision (better than 2.5 ppmv).

[7] As has been demonstrated in previous studies [O'Brien *et al.*, 1998], spectra of the O<sub>2</sub> A-band (0.76- $\mu\text{m}$ ) provide constraints on both the surface pressure and optical pathlength variations associated with the scattering by clouds/aerosols. The fact that the O<sub>2</sub> A-band contains both weak and strong lines provides the additional information on the altitude distribution of cloud/aerosols [Stephens and Heidinger, 2000]. We will limit our discussion to relatively clear sky conditions (scattering optical depth  $\tau_s < \sim 0.3$ , as determined from the O<sub>2</sub> band).

[8] The 0.76- $\mu\text{m}$  O<sub>2</sub> band spectra alone, however, are not adequate for characterizing the scattering by clouds/aerosols in the 1.58- $\mu\text{m}$  CO<sub>2</sub> band as cloud/aerosol optical properties can vary substantially with wavelength between the two bands. Although there is an O<sub>2</sub> band at 1.27  $\mu\text{m}$ , closer to the 1.58- $\mu\text{m}$  CO<sub>2</sub> band, it cannot be used for space-based O<sub>2</sub> observations as it produces intense, variable dayglow emission [Noxon, 1982].

[9] We therefore use the CO<sub>2</sub> band at 2.06  $\mu\text{m}$  in conjunction with the O<sub>2</sub> A-band to constrain the wavelength dependence of atmospheric scattering. This CO<sub>2</sub> band is sufficiently strong to be sensitive to scattering by cloud/aerosols. It also includes weak water vapor lines that can be used to provide direct constraints on humidity. On the other hand, since lines in the 2.06- $\mu\text{m}$  band are strongly saturated, this band is more susceptible to systematic errors, and must not be used with the O<sub>2</sub> band alone for CO<sub>2</sub> measurements.

<sup>1</sup>We can formally define  $X_{\text{CO}_2} = 0.2095 \times (\text{column CO}_2)/(\text{column O}_2)$ . The term vmr is used for dry air volume mixing ratio throughout this paper.

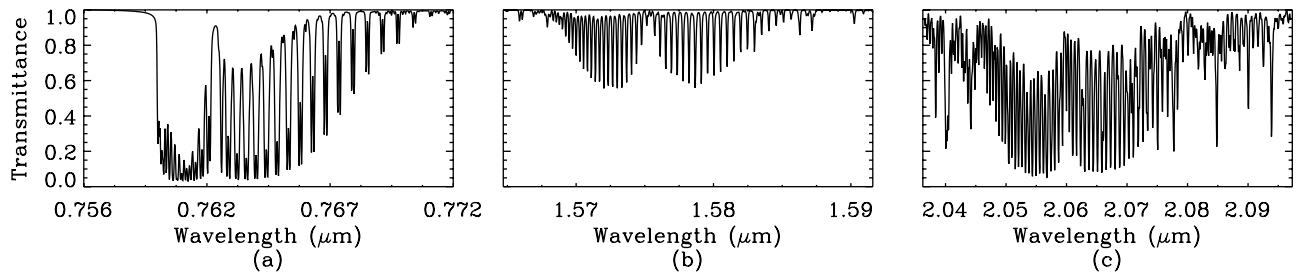


**Figure 1.** Simulated atmospheric transmission of the 0.76- $\mu\text{m}$  O<sub>2</sub> A-band (a), 1.58- $\mu\text{m}$  (b) and 2.06- $\mu\text{m}$  (c) CO<sub>2</sub> bands for standard midlatitude summer atmosphere, assuming a solar zenith angle (SZA) of 35° and a nadir viewing geometry.

[10] The spectral range of each spectrometer is chosen to cover the entire absorption band as well as some continuum at both ends of the band (Figure 1). The use of the entire band provides explicit constraints on the atmospheric temperature profile, because temperature affects strengths of the lines differently across the band in a well known manner. The continuum at edges of the bands provides additional information about the wavelength dependent optical properties of the surface and airborne particles. For our analysis, we assume the resolving power ( $R = \lambda/\Delta\lambda$ ) to be  $\sim 21,000$  for the CO<sub>2</sub> bands and  $\sim 17,500$  for the O<sub>2</sub> band. A small footprint ( $< 5 \text{ km}^2$ ) was assumed to increase the chance of observing the entire atmospheric column in the presence of patchy clouds. It also helps to minimize spatial inhomogeneities (clouds, surface topography, shorelines, etc.) within individual samples that could introduce errors in the retrievals. We consider only measurements with nadir viewing geometry in this study. Given the assumed resolving power and footprint size, we assume that the continuum signal to noise ratio (SNR) (the SNR in spectral regions without significant gaseous absorption) is  $\sim 400$  for the CO<sub>2</sub> bands and  $\sim 600$  for the O<sub>2</sub> band in each spectral sample and in each footprint when SZA is 35° and the surface albedo is  $\sim 6\%$ . This performance can be achieved with photon-noise limited detectors and current spectrometer technologies.

### 3. Retrieval Approach & Achievable Precisions

[11] The  $X_{\text{CO}_2}$  retrieval algorithm involves three major components. The first is a spectrum-resolving (line-by-line), multi-stream multiple scattering model for producing synthetic radiance spectra in scattering, absorbing atmospheres [Crisp, 1997]. Here, the same model was used to generate the “observed” spectrum and the “retrieved” spectrum. For both applications, the atmosphere was divided into 11 layers with 8 levels in the troposphere. The second component simulates the instrument’s spectral resolution, spectral range, sampling, wavelength-dependent line shape function, and throughput, as well as several instrument noise sources. The third component is an inverse method based on optimal estimation theory [Rodgers, 2000] for retrieving  $X_{\text{CO}_2}$  from the observed spectra. This model simultaneously retrieves several properties of the atmospheric and surface state  $\mathbf{x}$ , e.g. cloud, aerosol, temperature, humidity and surface pressure, albedo, as well as the CO<sub>2</sub> vmr.

[12] The function  $f(\mathbf{x})$  is used to denote the forward model, which includes the radiative transfer and the instrumental response components. The resulting synthetic spectra at the three selected bands simulate the measurements obtained from a single sounding, denoted as  $\mathbf{y}$ . The measurement process can thus be written as  $\mathbf{y} = f(\mathbf{x}) + \boldsymbol{\varepsilon}$  where  $\boldsymbol{\varepsilon}$  denotes the measurement error.

[13] We fit the three synthetic spectra simultaneously for the atmospheric/surface state using the optimal retrieval theory, which seeks to minimize the cost function

$$\chi^2 = [\mathbf{y} - f(\mathbf{x})]^T \mathbf{S}_\varepsilon^{-1} [\mathbf{y} - f(\mathbf{x})] + (\mathbf{x} - \mathbf{x}_a)^T \mathbf{S}_a^{-1} (\mathbf{x} - \mathbf{x}_a) \quad (1)$$

where  $\mathbf{x}_a$  is the a priori state,  $\mathbf{S}_a$  is the a priori covariance, and  $\mathbf{S}_\varepsilon$  is the measurement error covariance. We assume the measurement

errors to be Gaussian. We also assume that they are independent between pixels so that  $\mathbf{S}_\varepsilon$  is diagonal.

[14] A principal feature of the optimal retrieval theory is the use of a priori constraints, which represent the range of expected values for each parameter in the atmospheric state vector and the expected correlations between the parameters. For some variables, the a priori constraints can be estimated from existing climatological data (temperature, humidity profiles, and surface pressure) and model outputs (CO<sub>2</sub> profiles). For other properties, such as cloud and aerosol profiles, ad hoc constraints were constructed based on a Markov description of the profiles [Rodgers, 2000]. For the retrieval experiments presented here, we assumed that cloud/aerosols vary on a vertical scale height of about 200 mb, 500 mb and 300 mb in the planetary boundary layer (PBL), the free troposphere, and the stratosphere, respectively. The standard deviation in scattering optical depth of each of the 11 layers is assumed to be  $\sim 50\%$ , and to vary independently in the 2.06- $\mu\text{m}$  and 0.76- $\mu\text{m}$  bands. Scattering at 1.58  $\mu\text{m}$  is interpolated from those of the other two bands, with an assumed interpolation error of  $\sim 3\%$ . The validity of these assumptions is discussed at the end of this section. The band averaged albedos are considered to vary by  $\sim 30\%$  and are independent among the three bands. We assume no covariance between different quantities (e.g. between CO<sub>2</sub> and temperature).

[15] In our retrieval experiments, the forward model is linearized around each atmospheric/surface state, giving a weighting function matrix  $[K_{ij}] = \partial f_i / \partial x_j$ . Figure 2 shows the band averaged weighting function (i.e.  $\bar{K}_j = [\sum_i K_{i,j}^2 / \varepsilon_i^2]^{1/2}$ ) for CO<sub>2</sub> variations versus pressure levels, for cases with (solid line) and without (dashed line) atmospheric scattering. These weighting functions include contributions from both the 1.58- $\mu\text{m}$  and 2.06- $\mu\text{m}$  CO<sub>2</sub> bands. The sensitivity to CO<sub>2</sub> is maximum near the surface, where most CO<sub>2</sub> sources and sinks are located. In contrast, thermal IR techniques have poor sensitivity at low altitudes because the thermal contrast between the surface and the near-surface atmosphere is usually small [Engelen et al., 2001]. When atmospheric scattering is present, the sensitivity to low altitude CO<sub>2</sub> vmr decreases (dashed line in Figure 2).

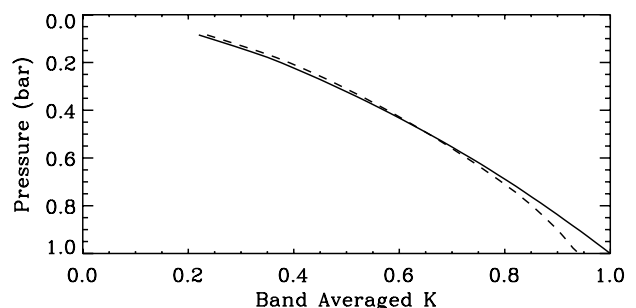


**Figure 2.** Band-averaged weighting function for CO<sub>2</sub> variations at different pressure levels with no atmospheric scattering (solid) and with  $\tau_s = 0.1$  (dashed). The weighting functions were scaled by the weight at 1 bar level when  $\tau_s = 0$ .

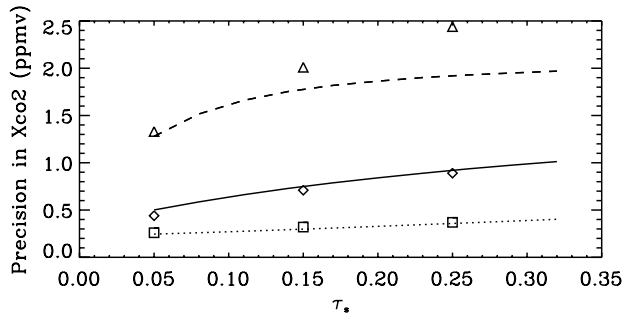


**Figure 3.** Achievable  $X_{\text{CO}_2}$  precisions calculated from linear covariance analysis versus the total scattering optical depth ( $\tau_s$ ) for SZA = 35° over the ocean (solid), over the land (dotted), and SZA = 75° over the ocean (dashed). The symbols ( $\Delta$ ,  $\diamond$  and  $\square$ ) represent the single sounding precisions obtained from retrieval experiments for a few selected cases. We have assumed that scattering at 1.58  $\mu\text{m}$  can be interpolated from the other two bands to  $\sim 3\%$  accuracy.

[16] A linear covariance analysis was conducted to study the achievable precisions. The posterior covariance for the state variables is

$$\mathbf{S} = \left( \mathbf{K}^T \mathbf{S}_e^{-1} \mathbf{K} + \mathbf{S}_a^{-1} \right)^{-1} \quad (2)$$

The quantity  $X_{\text{CO}_2}$  can be obtained by averaging the CO<sub>2</sub> profile, i.e.  $X_{\text{CO}_2} = \mathbf{h}^T \mathbf{x}$ , where  $\mathbf{h}$  is a vector that represents the vertical pressure-weighted averaging. The formal error variance in the retrieved  $X_{\text{CO}_2}$  is thus  $\mathbf{h}^T \mathbf{S} \mathbf{h}$ .

[17] Figure 3 shows the achievable precisions over the ocean (albedo is 0.06) for SZAs of 35° and 75° for a range of total scattering optical depth  $\tau_s$ . The precision worsens with increasing  $\tau_s$  and SZA. The former is due to the fact that most CO<sub>2</sub> variation is in the lower atmosphere, especially in the PBL. Increasing  $\tau_s$  thus decreases the sunlight that passes through this region and reduces the sensitivity to CO<sub>2</sub> changes there. The poorer precisions at high SZAs are mainly due to the reduced SNR, since less sunlight is intercepted by a unit area. For  $\tau_s$  between 0.05–0.30, the precision for a single sounding is about 0.4 to 0.9 ppmv for a SZA of 35° (solid), and about 1.3 to 2.5 ppmv for a SZA of 75° (dashed). The a priori error on  $X_{\text{CO}_2}$  is about 8 ppmv. If the 2.06- $\mu\text{m}$  CO<sub>2</sub> band is not used, the achievable precisions worsen by more than a factor of two (not shown). Similar estimates made for observations over land show better precisions, about 0.3–0.4 ppmv, (Figure 3, dotted line) because the higher albedo over land (a value of 0.2 was used) increases the SNR and reduces the relative contribution to the observed signal from light scattered by cloud/aerosols.

[18] Results from linear covariance analysis were tested against retrieval experiments. About 300 atmospheric/surface states were constructed consistent with the a priori constraints so that they cover the plausible climatological range. For each of the prescribed atmospheric/surface conditions, synthetic spectra were generated and subsequently retrieved for the atmospheric/surface state. Precisions were evaluated by comparing the retrieved quantities with the prescribed values. Results from a few such experiment are compared in Figure 3. The achieved precisions from these simulations agree well with the linear covariance estimates for cases with low cloud/aerosol loadings or low SZAs. At high SZAs and with high cloud/aerosol loadings, the achieved precisions from the retrieval experiments become worse than the linear covariance estimates, presumably associated with the increasingly nonlinear nature of the retrieval problem as scattering becomes more important.

[19] For a spaceborne CO<sub>2</sub> sensor in a high inclination orbit, thousands of soundings could be acquired on monthly to seasonal

time scales on spatial scales of 8° × 10°. Therefore, averaging large numbers of clear sky soundings will be possible except for regions with persistent overcast conditions, rendering random error negligible (Figure 4). Note that the random errors decrease at a rate slower than the square-root of the number of soundings, as the a priori errors tend to correlate with each other for nearby soundings. In Figure 4, we have assumed the a priori errors to be perfectly correlated so that they do not improve through averaging.

[20] Effects of wavelength-dependent surface albedo due to mineral features, plankton, etc. have been simulated by including in the state vector slow variations in the surface albedo of each band ( $\sim 30\%$ ) on the scale of  $\sim 3$  nm. We find that they do not significantly affect the achievable precision. This is expected because the spectral scale of the surface colors is much broader than that of the gaseous CO<sub>2</sub> features, and can be resolved explicitly in the continuum between the lines throughout each band. The effect of water vapor broadening of CO<sub>2</sub> lines was not tested in the above calculations. But these effects are reasonably well understood [Rosenmann *et al.*, 1988], and will be described in subsequent work. This factor should not significantly reduce the accuracy of  $X_{\text{CO}_2}$  retrievals because water vapor is well constrained by spectra acquired in the 2.06- $\mu\text{m}$  band.

[21] Although the a priori constraints used here were somewhat crude, they were sufficiently loose so that they did not excessively constrain the retrieval of  $X_{\text{CO}_2}$ . In the analysis of real satellite observations, these constraints can be improved by both establishing a more reliable climatology and using the preceding adjacent retrievals along the satellite so that the retrieval precisions will be further improved.

[22] The interpolation of scattering properties measured at 0.76  $\mu\text{m}$  and 2.06  $\mu\text{m}$  to 1.58  $\mu\text{m}$  warrants more discussion. For aerosols whose optical properties change slowly over this range of wavelengths (e.g. small sulfate particles, black carbon), interpolation by the simple Angstrom relation ( $\tau \propto \nu^n$ ) can be accurate to about a 1% level, even without a priori knowledge of the coefficient  $n$  or the actual aerosol type. Airborne particles whose optical properties do not change uniformly with wavelength, however, need to be typed in order to do an accurate interpolation. The high resolution measurements provide additional constraints on the particle type. For instance, the 2.06- $\mu\text{m}$  band and the 1.58- $\mu\text{m}$  band are on the edge of strong water ice absorption features. A thin cirrus ice cloud can thus be clearly identified since it produces a significant slope in the continuum and also changes the shapes of the cores of saturated lines. Ubiquitous airborne dust and long-lived soluble aerosols pose special problems as they have variable compositions and size distributions that can yield a range of spectral signatures at NIR wavelengths. The identification and characterization of these aerosols warrants further investigation. We have assumed that scattering at 1.58  $\mu\text{m}$  can be interpolated from the other two bands with an accuracy of  $\sim 3\%$ . A different

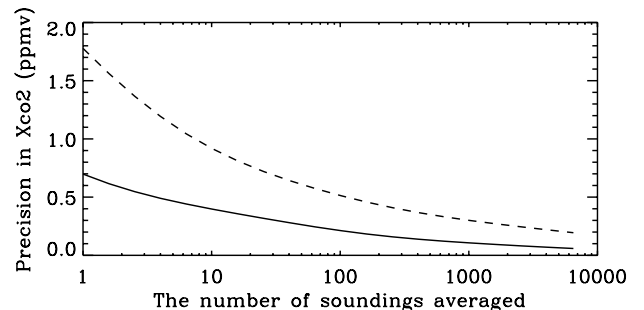


**Figure 4.** Precisions of  $X_{\text{CO}_2}$  retrievals as a function of the number of soundings averaged for SZA = 35° (solid) and 75° (dashed). Both cases assume a surface albedo of 0.06 and a total scattering optical depth of about 0.15.

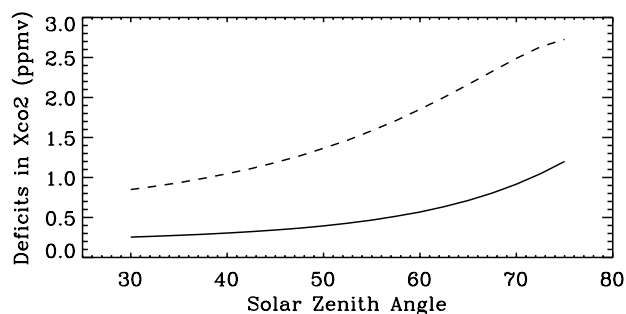


**Figure 5.** Deficits in  $X_{CO_2}$  due to a constant zero offset error over the ocean (surface albedo of 0.06, dashed line) and over the land (surface albedo of 0.2, solid line) as a function of SZA. The zero offset error is 0.2% of the continuum level for an albedo of 0.06 at 35° SZA. All cases have a total scattering optical depth  $\sim 0.05$ .

choice of the interpolation error, e.g. 10% or 1%, worsens or improves the achievable precision by less than 20–30%.

#### 4. Systematic Errors and Potential Biases

[23] The preceding analysis assumes that the forward model is perfect. In practice, there will inevitably be inadequacies in the representation of the characteristics of the instrument (e.g. uncertainties in the instrument line shape, zero offset, detector non-linearity, polarization etc.), and in the atmospheric radiative transfer (e.g. errors in the gas absorption line database, oversimplifications in the treatment of radiative transfer). These inadequacies will introduce systematic errors in the  $X_{CO_2}$  measurements. For the purpose of characterizing the carbon sources and sinks, it is critical that the measurements are free of spatially and temporally coherent biases, i.e. systematic errors that vary with geographic location, SZA, or surface type. As an example of such a systematic error, we consider the effect of an uncorrected zero offset error due to excess dark current in the detector of the 1.58- $\mu\text{m}$  region. This error adds a constant radiance offset to each spectrum, decreasing the fractional depths of the CO<sub>2</sub> absorption lines. The magnitude of the induced systematic error depends on the absorption depth of the CO<sub>2</sub> lines and the continuum radiance level; the former varies with SZA and the latter varies with both surface albedo and SZA. For dark surfaces or high SZAs, the signal gets weaker, and the error induced in  $X_{CO_2}$  gets larger, as shown in Figure 5. Since surface albedo is typically much larger over land than ocean, a given zero level offset error would reduce the  $X_{CO_2}$  less over land than over ocean, resulting in a spurious oceanic sink of CO<sub>2</sub>. Similarly, since the high latitude observations are generally made at higher solar zenith angles than the low latitude observations, the zero level offset error would reduce the  $X_{CO_2}$  less in the tropics than in the polar regions, leading to a spurious high latitude CO<sub>2</sub> sink.

[24] Fortunately, there are two factors that mitigate the impact of the systematic errors: 1) In the high-resolution, spectrometric approach, many types of systematic errors will produce distinctive spectral signatures. The high SNR that is attainable using reflected NIR sunlight facilitates the detection of these residuals, and provides the information needed to deduce their origin and test the efficacy of any corrections. 2) Validation experiments that combine accurate ground-based and airborne CO<sub>2</sub> profiling capabilities provide an effective way for identifying and quantifying biases with large spatial scales. While the amplitude of systematic errors will vary with location, their sources will vary slowly in many cases (as in the zero offset example). Such errors can be corrected by careful calibration and validation measurements.

[25] Sampling biases may also affect the inference of carbon sources and sinks, even if the  $X_{CO_2}$  retrievals are perfect. For instance, the solar NIR method only measures  $X_{CO_2}$  during the

day under clear-sky conditions. However, in many ecosystems, photosynthesis is stronger in these conditions such that the measured  $X_{CO_2}$  could be lower than average. To mitigate the impact of such sampling errors, the space based  $X_{CO_2}$  measurements must be combined with time-resolved in-situ data, and analyzed with chemical tracer transport models that properly account for the sampling conditions. Such models are being developed [Rayner et al., 2002].

#### 5. Summary and Conclusions

[26] We have introduced a method of measuring  $X_{CO_2}$  from space using high resolution NIR spectrometry of reflected sunlight through the simultaneous use of the CO<sub>2</sub> (1.58- $\mu\text{m}$  and 2.05- $\mu\text{m}$ ) and O<sub>2</sub> (0.76- $\mu\text{m}$ ) bands. Using prototype retrieval simulations based on a practical satellite instrument design, we show that it is possible to retrieve  $X_{CO_2}$  to precisions of  $\sim 0.3$ –2.5 ppmv from a single clear sky sounding ( $\tau_s < \sim 0.3$ ) for a range of atmospheric and surface conditions. Thousands of such soundings are expected at regional scales on monthly intervals, and can be combined to reduce the effects of random measurement errors over all but the most persistently cloudy regions. The main challenge is therefore to avoid systematic measurement errors which can introduce geographically dependent biases. These factors highlight the need for a careful calibration and validation program, designed to identify and eliminate these biases. We conclude that the 3-band, high-resolution, spectrometric approach using NIR reflected sunlight has the potential for highly accurate  $X_{CO_2}$  measurements.

[27] **Acknowledgments.** We thank two anonymous referees and members of the OCO Team for valuable comments. This research was supported in part by a NASA grant to the Jet Propulsion Laboratory and the Caltech President's Fund. ZMK and YLY were supported by NASA grants NAG5-7230, NAG1-1806 to Caltech.

#### References

- Crisp, D., Absorption of sunlight by water vapor in cloudy conditions: A partial explanation for the cloud absorption anomaly, *Geophys. Res. Lett.*, **24**, 571–574, 1997.
- Engelen, R. J., A. S. Denning, K. R. Gurney, and S. G. L., Global observations of the carbon budget. 1. Expected satellite capabilities for emission spectroscopy in the EOS and NPOESS eras, *J. Geophys. Res.*, **106**, 20,055–20,068, 2001.
- IPCC, *Intergovernmental Panel on Climate Change Assessment: Climate Change 1995*, pp. 73, 1996.
- Noxon, J. F., A global study of O<sub>2</sub> 1-delta Airglow-Day and twilight, *Planet Space Sci.*, **30**, 545–557, 1982.
- O'Brien, D. M., R. M. Mitchell, S. A. English, and G. A. Da Costa, Airborne Measurements of air mass from O<sub>2</sub> A-band absorption spectra, *J. Atmos. Oceanic Technol.*, **15**, 1272–1286, 1998.
- Rayner, P. J., and D. M. O'Brien, The utility of remotely sensed CO<sub>2</sub> concentration data in surface source inversions, *Geophys. Res. Lett.*, **28**, 175–178, 2001.
- Rayner, P. J., R. N. Law, D. M. O'Brien, T. M. Butler, and M. Dilley, Global observations of the carbon budget: III Initial assessment of the impact of satellite orbit, scan geometry and cloud on measuring CO<sub>2</sub> from space, *J. Geophys. Res.*, in press, 2002.
- Rodgers, C. D., *Inverse methods for atmospheric sounding: Theory and practice*, 238 pp., World Scientific, Inc., 2000.
- Rosenmann, L., J. M. Hartmann, M. Y. Perrin, and J. Taine, Accurate calculated tabulations of IR and Raman CO<sub>2</sub> line broadening by CO<sub>2</sub>, H<sub>2</sub>O, N<sub>2</sub>, O<sub>2</sub> in the 300–2400K temperature range, *Appl. Optics*, **27**, 3902–3907, 1988.
- Sarmiento, J. L., and S. C. Wofsy, A U. S. Carbon Cycle science plan, 1999.
- Stephens, G. L., and A. Heidinger, Molecular line absorption in a scattering atmosphere. Part I: Theory, *J. Atmos. Sci.*, **57**, 1599–1614, 2000.

Z. Kuang and Y. Yung, Division of Geological and Planetary Sciences, Caltech, Pasadena, CA 91125, USA. (kzm@gps.caltech.edu)  
J. Margolis, G. Toon, and D. Crisp, Jet Propulsion Laboratory, California Institute of Technology, Pasadena, CA, USA.